Macromolecules
ARTICLE

Macromolecules **2010**, *43*, 7151–7158 **7151**
DOI: 10.1021/ma101243s

Synthesis of New Star-Shaped Polymers with Styrene−Fluorene Conjugated Moieties and Their Multicolor Luminescent Ordered Microporous Films

Jung-Ching Hsu,[†] Kenji Sugiyama,[‡] Yu-Cheng Chiu,[†] Akira Hirao,*[,‡] and Wen-Chang Chen*[,†,§]

[†]Department of Chemical Engineering, National Taiwan University, Taipei 10617, Taiwan, [‡]Department of Organic and Polymeric Materials, Tokyo Institute of Technology, 2-12-1 Ookayama, Meguro-ku, Tokyo 152-8552, Japan, and [§]Institute of Polymer Science and Engineering, National Taiwan University, Taipei 10617, Taiwan

Received June 3, 2010; Revised Manuscript Received July 19, 2010

ABSTRACT: We report the synthesis, photophysical properties, and morphology of new star-shaped polymers with styrene−fluorene (St-Fl) conjugated moieties. Three polymers with different number of arms ($(P(St\text{-}Fl)_n$, $n = 3$, 4, and 8) were obtained by living anionic polymerization, and they exhibited a narrow molecular weight distribution ($M_n/M_w < 1.06$). The effects of arm numbers, humidity, and solution concentration on the formation of the microporous structures were studied. It was found that the high molecular weight $P(St\text{-}Fl)_8$ could form a highly ordered microporous film via drop-casting, but not on the polymers with the other two arm numbers. In addition, the pore diameter was reduced while enhancing solution concentration or decreasing humidity. Relatively uniform blue-emitting characteristics were obtained on the $P(St\text{-}Fl)_8$ microporous films. Such highly ordered structure led to a red shift in photophysical properties, such as absorption and photoluminescence. Furthermore, green- and red-emission microporous films were obtained via blending a relatively small amount (∼1%) of poly((9,9-dioctylfluorenyl-2,7-diyl)-*co*-(1,4-benzo-(2,1′,3)-thiadiazole) or bis(1-phenylisoquinoline)(acetylacetonate)irdium(III) ($Ir(piq)_2(acac)$) through efficient energy transfer. The experimental results suggested a new approach to synthesis of star-branched polymers with pendant conjugated moieties and the formation of the multicolor ordered microporous films.

Introduction

Highly ordered microporous films have potential applications in photonic band gap,[1,2] cell patterning,[3] filtration membranes,[4] and surface wettability.[5,6] The common methodology of preparing such microporous films involves water vapor condensed on the solution surface and forms ordered hole array structures during solvent evaporation.[7−10] Linear polymers with end-functionalized groups, star-shaped polymers, and rigid-rod polymers were employed to obtain the ordered microporous films.[7] The pore size was controlled by the polymer solution concentration, polymer structure or architecture, the molecular weight, and the casting condition (such as solvent, concentration, and humidity, etc.).[11]

Recently, conjugated polymer-based microporous films have attracted significant scientific interest because of the potential applications in photonic band gap[1,2] and optoelectronic devices.[12−16] Several conjugated polymers were reported to form a highly ordered hole array structure,[17−20] including poly(*p*-phenyleneethynylene), poly(3-alkylthiophene), poly(9,9′-dialkylfluorene), poly(*p*-phenylenevinylene) (PPV), and hyperbranched poly(phenylenevinylene). On the other hand, star-shaped polymers with side chain conjugated quinoline moiety were found to form ordered microporous structure with green emission, which were prepared by reversible addition−fragmentation chain transfer (RAFT) polymerization.[21] In general, the star-shaped polymer could generate a higher degree of ordering than the linear polymer analogue due to their ability to precipitate instantaneously at the solution/water interface.[9,22−27] We have employed the living anionic polymers were widely used to synthesize well-defined star-branched polymers with a relatively low polydispersity index.[28,29] However, the synthesis of star-shaped polymers with pedant conjugated moieties by living anionic polymerization has not been explored yet. In addition, it requires a new methodology to develop a multicolor microporous structure based on such star-shaped polymers.

In this study, we report the synthesis, properties, and ordered microporous structure of new star-shaped polymers with styrene−fluorene (St-Fl) moieties using living anionic polymerization. The linear polymer arm was first prepared from the monomer of St-Fl and then used to synthesize the star-branched polymers through the arm-first approach via the different number functional core ($BnBr_n$), as shown in Scheme 1. The photophysical properties of the prepared films were investigated by optical absorption and photoluminescence (PL) spectra. Highly ordered microporous film was prepared from the star-branched polymers by the breath figure method.[7,10] The effects of arm numbers, humidity, and concentration on the formation of ordered porous film were studied. The morphology was characterized by field-emission scanning microscope (FE-SEM), atomic force microscope (AFM), and laser confocal microscope (Confocal). The experimental results showed that the eight-arm star-shaped polymer ($P(St\text{-}Fl)_8$) easily formed highly ordered microporous morphology, which showed blue emission. Besides, multicolor

---

*To whom all correspondence should be addressed: Tel +81-3-5734-2131, Fax +81-3-5734-2887, e-mail ahirao@polymer.titech.ac.jp (A.H.); Tel +886-2-23628398, Fax +886-2-23623040, e-mail chenwc@ntu.edu.tw (W.-C.C.).

Scheme 1. Synthesis of the Star-Shaped Polymers Using Different Numbers of BnBr Functional Core

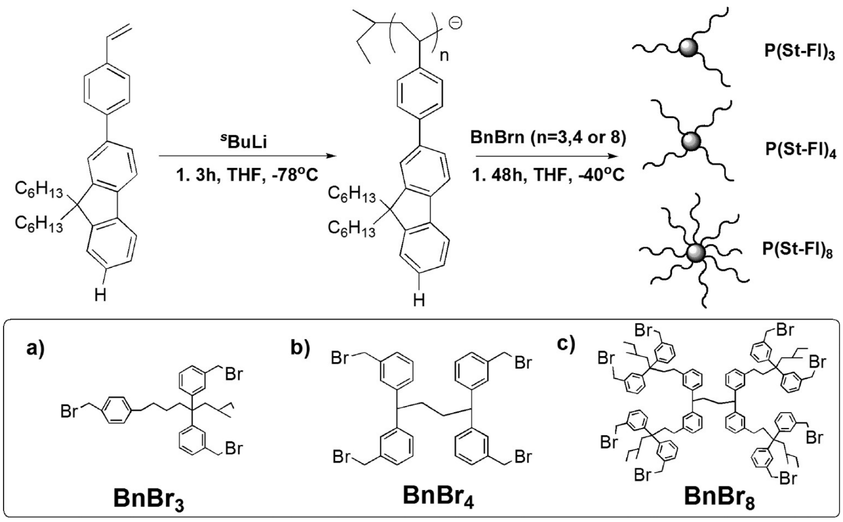

Table 1. Anionic Polymerization of P(St-Fl)$_n$ in THF[a]

run	*s*-BuLi (mmol)	monomers (BnBrn/St-Fl) (mmol)	arm (M_n) calc	arm (M_n) obs[b]	star-shaped polymer (M_n) calc[c]	star-shaped polymer (M_n) obs[b]	M_w/M_n[b]
P(St-Fl)$_3$	0.150	0.0235/2.59	7410	9070	27600	27700	1.02
P(St-Fl)$_4$	0.165	0.0244/4.43	12700	11600	46800	56500	1.06
P(St-Fl)$_8$	0.191	0.0157/4.42	10800	12300	99900	98200	1.02

[a] Yields of polymers were always quantitative. [b] Determined by SEC-RALLS. [c] Calculated molecular weight of the star-shaped polymer = (observed molecular weight of the arm) × arm number + molecular weight of the core.

emission of the microporous films could be obtained through the energy transfer between the prepared star-shaped polymer and commercial conjugated materials, poly((9,9-dioctylfluorenyl-2,7-diyl)-*co*-(1,4-benzo-(2,1′,3)-thiadiazole) (ADS233YE) or bis(1-phenylisoquinoline)(acetylacetonate)iridium(III) (Ir(piq)$_2$(acac)).

Experimental Section

Materials. All the reagents were purchased from Aldrich (St. Louis, MO) or Acros Organics (Geel, Belgium) and used as received. The monomer, styrene para-substituted with the fluorene moiety (St-Fl),[30] and the BnBr$_n$ (n = 3, 4, or 8) core compounds were synthesized according to the literature.[28,31] Poly((9,9-dioctylfluorenyl-2,7-diyl)-*co*-(1,4-benzo-(2,1′,3)-thiadiazole) (ADS233YE) and bis(1-phenylisoquinoline)(acetylacetonate)-irdium(III) (Ir(piq)$_2$(acac)) were purchased from American Dye Source Inc. (Quebec, Canada). Tetrahydrofuran (THF) was refluxed over sodium wire, distilled over $LiAlH_4$ under nitrogen, and then distilled from its sodium naphthalenide solution under high-vacuum conditions (10^{-6} Torr). *sec*-Butyllithium (*s*-BuLi, 1.4 M in heptane, Aldrich, Japan) was used as received.

General Procedure for the Synthesis of Star-Shaped Polymers, P(St-Fl)$_n$ (n = 3, 4, or 8). The star-shaped polymer P(St-Fl)$_3$ was prepared by the sequential addition of St-Fl, *s*-BuLi, and multifunctional BnBr$_3$ core, as shown in Scheme 1. Afterward, the reaction was quenched with degassed methanol. The first-stage polymerization was carried out at −78 °C by mixing St-Fl (2.59 mmol) in THF solution (16.6 mL) with *s*-BuLi (0.150 mmol) in heptane solution (2.3 mL). The reaction mixture was allowed to stand for 3 h. Then, a small portion of the reaction solution was taken out from the reaction mixture in order to determine the molecular weight of the arm. Functional BnBr$_3$ core (0.0235 mmol) in THF solution (3.9 mL) was added to the reaction reactor, and the reaction temperature changed to −40 °C for an additional 48 h. The mole ratio of the living anionic polymer chain end was used excess relative to the benzyl bromide moieties. Finally, the reaction mixture was quenched with degassed methanol and concentrated by using rotary evaporator to dry. The star-shaped polymer was isolated by fractional precipitation using THF−methanol to remove excess linear polymer and further freeze-dried from its absolute benzene solution. The GPC trace of star-shaped polymer is shown in Figure S1. An isolated polymer with white powder product yield was 25%. The polymer was characterized by SEC-RALLS, ^{1}H NMR, and element analysis. ^{1}H NMR (500 MHz, CD_2Cl_2-d_2, δ): 6.3−7.6 (broad, aromatic), 2.3−1.2, 1.1−0.3 (broad, $-C_6H_{13}$, aliphatic chain of the core). Molecular weight distribution (GPC): M_n = 27 700, PDI = 1.02. Anal. Calcd: C, 90.76%; H, 9.24%. Found: C, 89.12%; H, 9.43%.

The syntheses of P(St-Fl)$_4$ and P(St-Fl)$_8$ were carried out with multifunctional BnBr$_4$ and BnBr$_8$ cores under the same conditions. The specific amount of initiator and monomers added in the reaction and the molecular weight measured by SEC-RALLS are listed in Table 1. The characterization results for the two polymers are described as follows:

P(St-Fl)$_4$. A white powder product with the isolated yield of 29%. ^{1}H NMR (500 MHz, CD_2Cl_2-d_2, δ): 6.3−7.6 (broad, aromatic), 2.1−1.2, 1.1−0.3 (broad, backbone, $-C_6H_{13}$, aliphatic chain of the core). Molecular weight distribution (GPC): M_n = 56 500, PDI = 1.06. Anal. Calcd: C, 90.77%; H, 9.23%. Found: C, 89.93%; H, 9.32%.

P(St-Fl)$_8$. A white powder product with the yield of 21%. ^{1}H NMR (500 MHz, CD_2Cl_2-d_2, δ): 6.4−7.8 (broad, aromatic), 2.1−1.3, 1.1−0.4 (broad, $-C_6H_{13}$, aliphatic chain of the core). Molecular weight distribution (GPC): M_n = 98 200, PDI = 1.02. Anal. Calcd: C, 90.74%; H, 9.26%. Found: C, 90.02%; H, 9.30%.

Preparation of Highly Ordered Microporous Films. Star-shaped polymers, P(St-Fl)$_3$, P(St-Fl)$_4$, and P(St-Fl)$_8$, were dissolved in CS_2 solutions with the concentration of 10 g L^{-1}. The polymer solution was cast onto the quartz substrate under ambient conditions with adequate air flow to yield the microporous films at room temperature (22 °C). The opaque film was

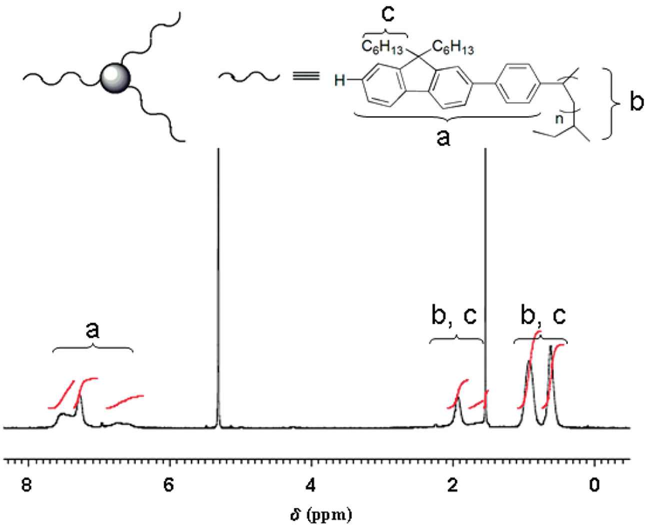

Figure 1. ^{1}H NMR spectra of the P(St-Fl)$_3$ star-shaped polymer.

observed on quartz surface after all solvents were evaporated. Relative humidity was measured under ambient conditions. Spin-coating of the film was performed at a rate of 1000 rpm.

Characterization. ^{1}H NMR spectra of the polymer solution were measured on a Bruker Avance 500 NMR in CD_2Cl_2. Size exclusion chromatography (SEC) was performed on an Asahi Techneion AT-2002 equipped with a Viscotek TDA model 302 triple detector array using THF as a carrier solvent at a flow rate of 1.0 mL min^{-1} at 30 °C. Three polystyrene gel columns of pore sizes (650, 200, and 75 Å) (bead size 9 μm) were used.

Thermal analysis of the polymers were characterized by a TA Instruments TGA 951 thermogravimetric analyzer (TGA) at a heating rate of 20 °C min^{-1} under a nitrogen atmosphere from room temperature to 800 °C. Differential scanning calorimetry (DSC) measurements were proceed under a nitrogen atmosphere at a heating rate of 10 °C min^{-1} from −30 to 200 °C using a TA Instruments Q-20.

The morphology of the microporous film was characterized by field-emission scanning electron microscopy (FE-SEM) (JEOL JSM-6330F). The images were taken using a microscope operated at an accelerating voltage of 15 kV. Before imaging, the samples were sputtered with Pt. Atomic force micrographs (AFM) images were obtained with a Nanoscope 3D Controller AFM (Digital Instruments) operated in the tapping mode at room temperature. Relative humidity was measured by a CRECER hygrometer. UV−vis optical absorption and photoluminescence (PL) spectra were obtained using a Hitachi U-4100 spectrometer and a Fluorolog-3 spectrofluorometer (Jobin Yvon), respectively. Fluorescence optical microscope images were taken using a two-photon laser confocal microscope (Leica LCS SP5).

Results and Discussion

Synthesis and Characterization of Star-Shaped Polymers. Figure 1 shows the ^{1}H NMR spectra of P(St-Fl)$_3$ in CD_2Cl_2. The peaks around 6.3−7.6 ppm are assigned to the protons on aromatic ring, while those at 2.3−0.3 ppm are attributed to the protons on alkyl side chain of the fluorene, the ethylene backbone unit, and aliphatic chain of the benzyl bromide core. The ^{1}H NMR spectra of the other two polymers also exhibit the proton peaks consistent with the proposed structure, as shown in Figures S2 and S3. The number-average molecular weight (M_n) and polydispersity index (PDI) of P(St-Fl)$_3$, P(St-Fl)$_4$, and P(St-Fl)$_8$ determined by SEC-RALLS are shown in Figure S1 and summarized in Table 1. The molecular weights and polydispersity index (PDI) of P(St-Fl)$_3$, P(St-Fl)$_4$, and P(St-Fl)$_8$ are (M_n = 27 700, PDI = 1.02), (M_n = 56 500, PDI = 1.06), and (M_n = 98 200, PDI = 1.02), respectively. All of the three star-shaped polymers show narrow molecular weight distribution (M_n/M_w < 1.06). The arm number is estimated by comparing the SEC-RALLS results of the star-shaped polymer with that of the polymer arm only. The three-, four-, and eight-arm star-shaped polymers, P(St-Fl)$_3$, P(St-Fl)$_4$, and P(St-Fl)$_8$, were successfully synthesized using the cores of $BnBr_3$, $BnBr_4$, and $BnBr_8$, respectively. The successive arm numbers of three to eight render the opportunity to systematically study their resulted morphologies of the star-shaped polymers. The elemental analyses on the carbon and hydrogen contents of the three star-shaped polymers are in a good agreement with the theoretical compositions. The above results suggest the successful preparation of the target star-shaped polymers.

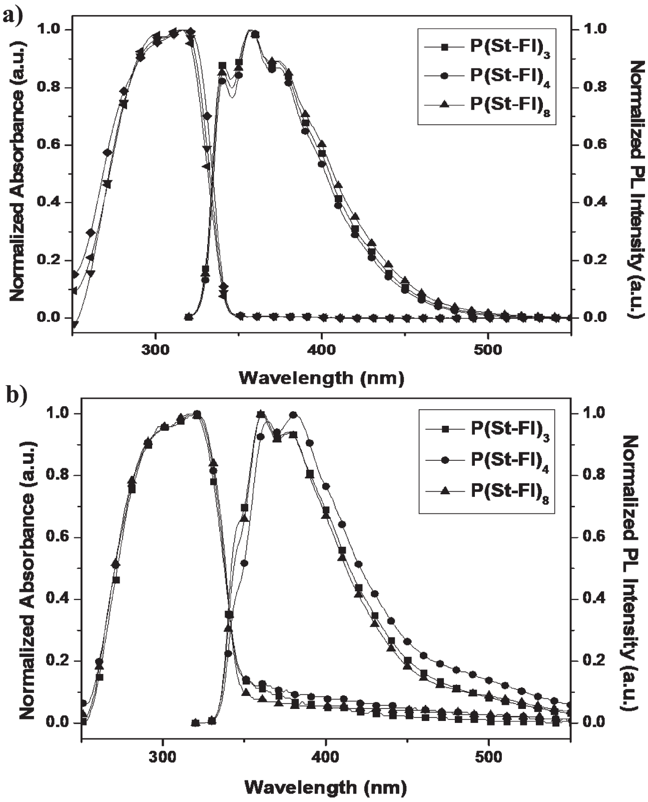

Figure 2. UV−vis absorption and photoluminescent spectra of the studied star-shaped polymers: (a) in THF solution and (b) thin films.

The prepared polymers are very soluble in common organic solvents, such as CH_2Cl_2, $CHCl_3$, THF, toluene, etc., which could be used to prepare uniform films. Figure S4(a) in the Supporting Information shows the thermogravimetric curves of the of the studied polymers, P(St-Fl)$_3$, P(St-Fl)$_4$, or P(St-Fl)$_8$, under a nitrogen atmosphere, which exhibits the thermal decomposition temperatures (T_d, 10% weight loss temperature) of 368, 405, and 409 °C, respectively. The glass transition temperatures (T_g) of P(St-Fl)$_3$, P(St-Fl)$_4$, or P(St-Fl)$_8$ are observed at 63, 88, and 95 °C, respectively, as observed from the DSC curves in Figure S4(b) in the Supporting Information. The enhanced thermal stability as the arm number increased is probably due to the higher molecular weight of the P(St-Fl)$_8$ polymer among the studied polymers. In addition, the prepared polymers also have good thermal stability for practical applications, as shown in Figure S4.

Figures 2a and 2b shows the optical absorption and photoluminescence (PL) spectra of the star-shaped polymers

Table 2. Photophysical Properties of $P(St\text{-}Fl)_3$, $P(St\text{-}Fl)_4$, and $P(St\text{-}Fl)_8$

materials	UV−vis λ_{max}^{abs}, solution (nm)[a]	UV−vis λ_{max}^{abs}, film (nm)	PL λ_{max}^{PL}, solution (nm)[a]	PL λ_{max}^{PL}, film (nm)
$P(St\text{-}Fl)_3$	299, 316	303, 320	341, 358	361, 378
$P(St\text{-}Fl)_4$	299, 317	301, 321	341, 358	364, 381
$P(St\text{-}Fl)_8$	299, 316	303, 320	341, 358	361, 378
P(St-Fl)[b]	296, 313	300, 317	342, 358	365, 384

[a] In THF dilute solution. [b] Result from ref 30.

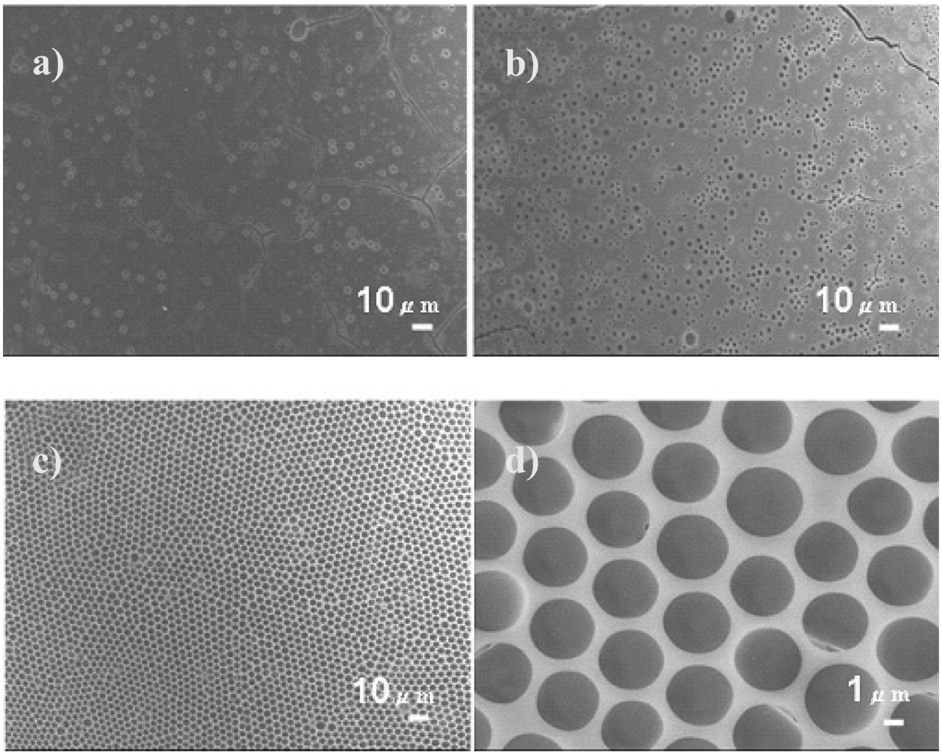

Figure 3. SEM images: (a) $P(St\text{-}Fl)_3$; (b) $P(St\text{-}Fl)_4$; (c) $P(St\text{-}Fl)_8$ drop-casting thin film prepared from the solution concentration of 10 g L^{-1}at the relative humidity of 80%. The magnified SEM image of $P(St\text{-}Fl)_8$ is shown in (d).

$P(St\text{-}Fl)_3$, $P(St\text{-}Fl)_4$, and $P(St\text{-}Fl)_8$ in THF and film, respectively. The absorption peak maxima of the three polymers are 316−317 and 320−321 nm for the solution and film, respectively, which shows insignificant variation with the arm number. The above absorption or emission band is attributed to the π−π^* transition of the styrene−fluorene moiety. The PL peak maxima of the three polymers in THF are observed at similar wavelengths of 341 and 358 nm, while those of thin films exhibit two peak maxima at 361−364 and 378−381 nm, respectively. The above photophysical properties of the studied polymers are summarized in Table 2. The obtained absorption and PL peak maxima exhibit insignificant variation with the arm number and are very close to that of the analogous linear polymer. It suggests the interchain interaction or polymer aggregation is relatively limited since only one conjugated styrene−fluorene moiety on the polymer side chain.

Morphology of the Polymer Films. Figure 3 illustrates the SEM images of three films prepared from CS_2 solution (10 g L^{-1}) at a relative humidity of 80%. Nonordered porous structure was obtained for $P(St\text{-}Fl)_3$ and $P(St\text{-}Fl)_4$ thin films. However, highly ordered microporous structure is observed on the $P(St\text{-}Fl)_8$ thin film, which has the pore size around 3.2 μm. Note that there is no ordered morphology from the linear homopolymer, P(St-Fl) (M_n = 18 430, PDI = 1.02) under a similar preparation condition, as shown in Figure S5. The star-shaped polymer, $P(St\text{-}Fl)_8$, has a higher molecular weight and segment density (more compact structure) than the other two star-shaped polymers, $P(St\text{-}Fl)_3$ and $P(St\text{-}Fl)_4$. Thus, it could precipitate at the solution/water interface easily, which leads to the formation of the solid polymer envelope before the water droplet coalescence occurred.[10] Figure S6 shows the photography of the star-shaped polymers of $P(St\text{-}Fl)_n$ (n = 3, 4, or 8) in CS_2 solution (10 g L^{-1}) by adding the same amount of water (1 mL). Only the vial of $P(St\text{-}Fl)_8$ changes to a turbid solution, suggesting that $P(St\text{-}Fl)_8$ easily precipitates at the solution/water interface.

Figures 4a, 4b, and 4c show the microporous film of $P(St\text{-}Fl)_8$ prepared from different concentrations of 10, 20, and 50 g L^{-1} in CS_2 at a relative humidity of 75%, respectively, which have the average pore sizes of 3.0, 2.3, and 1.9 μm. The reducing pore size at a higher polymer concentration is probably due to the difficulty growing or coalescing for the water droplets. The drop-cast thin films in Figure 4 show the highly ordered microporous structures. However, the spin-coated thin film exhibits a relatively smooth surface without the ordered structure, as shown in Figure S7, which is probably due to the fast evaporation of the solvent. Figures 5a and 5b show the AFM images of the $P(St\text{-}Fl)_8$ film prepared from the solution (20 g L^{-1}) at the relative humidity of 75%, which clearly exhibits an ordered open pore structure on the quartz surface. In addition, the pore size of the $P(St\text{-}Fl)_8$ microporous film slightly reduces from 3.2 to 3.0 μm as the relative humidity decreases from 80 to 75%. However, no ordered structure is observed at a relative humidity of 55%. It suggests the importance of the

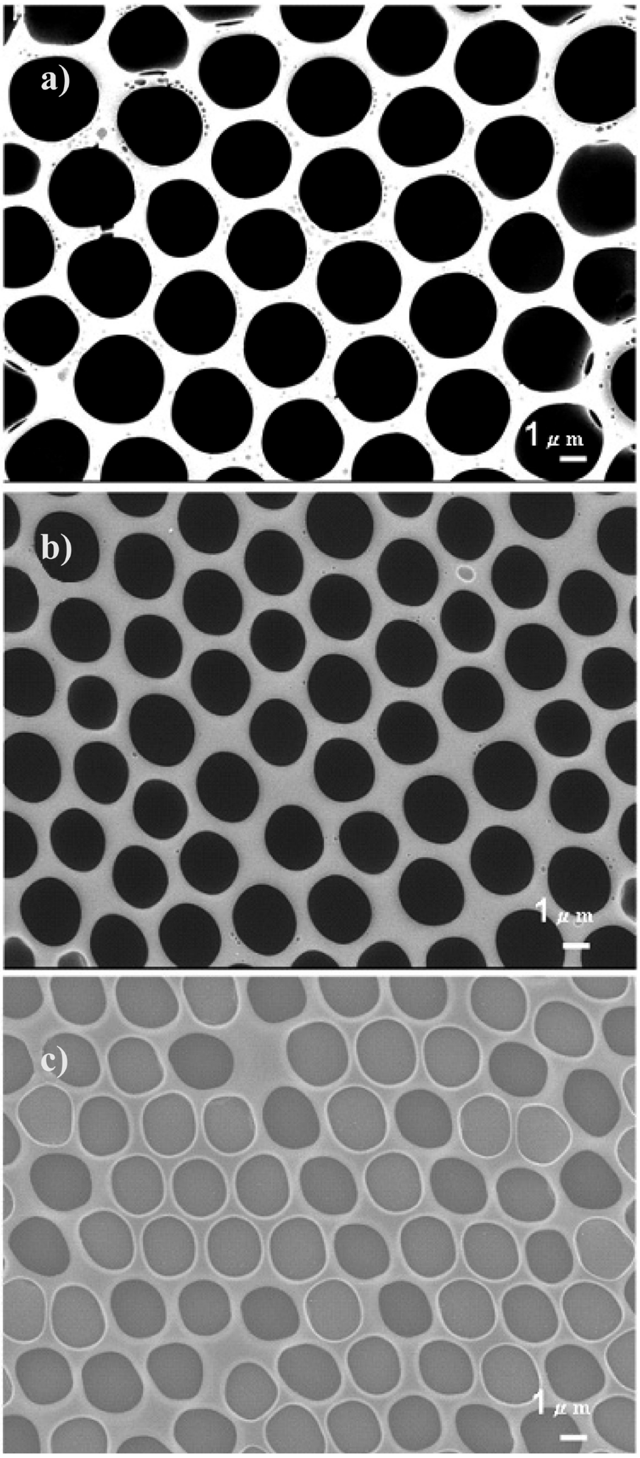

Figure 4. SEM images of P(St-Fl)$_8$ drop-casting thin films prepared from different concentrations of (a) 10, (b) 20, and (c) 50 g L^{-1} at the relative humidity of 75%.

relative humidity on the formation of ordered microporous structures.

The mechanism on forming the water-assisted ordered microporous structure on the drop-cast P(St-Fl)$_8$ is proposed in Figure 6, similar to that reported in the literature.[7,10] When the solvent evaporated in the humid environment, the water vapor on the solvent surface coalesced immediately due to the rapid cooling on the solvent/water surface interface. The polymer could be precipitated on the water/solution interface instantly and form a solid

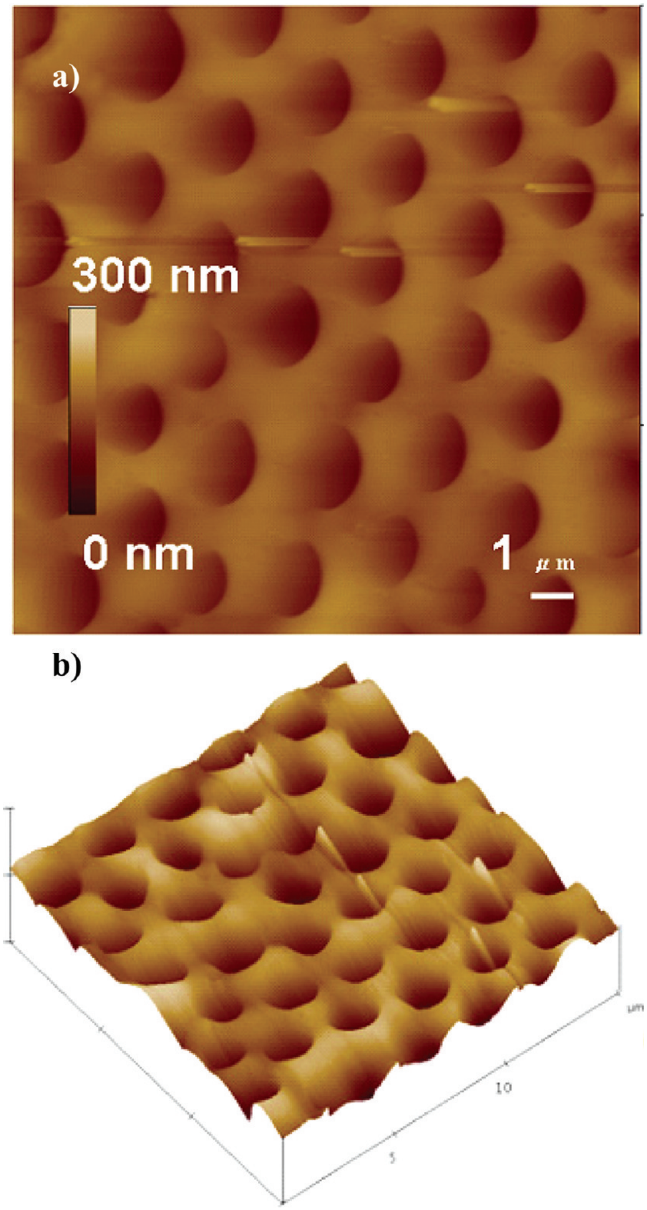

Figure 5. (a) Height images of the P(St-Fl)$_8$ drop-casting film on quartz substrate. (b) 3D image of the microporous film.

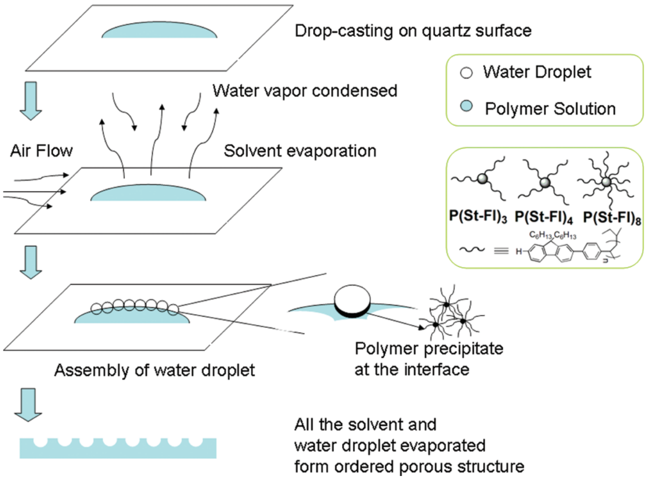

Figure 6. Proposed mechanism on the formation of the ordered microporous film from the prepared star-shaped polymers.

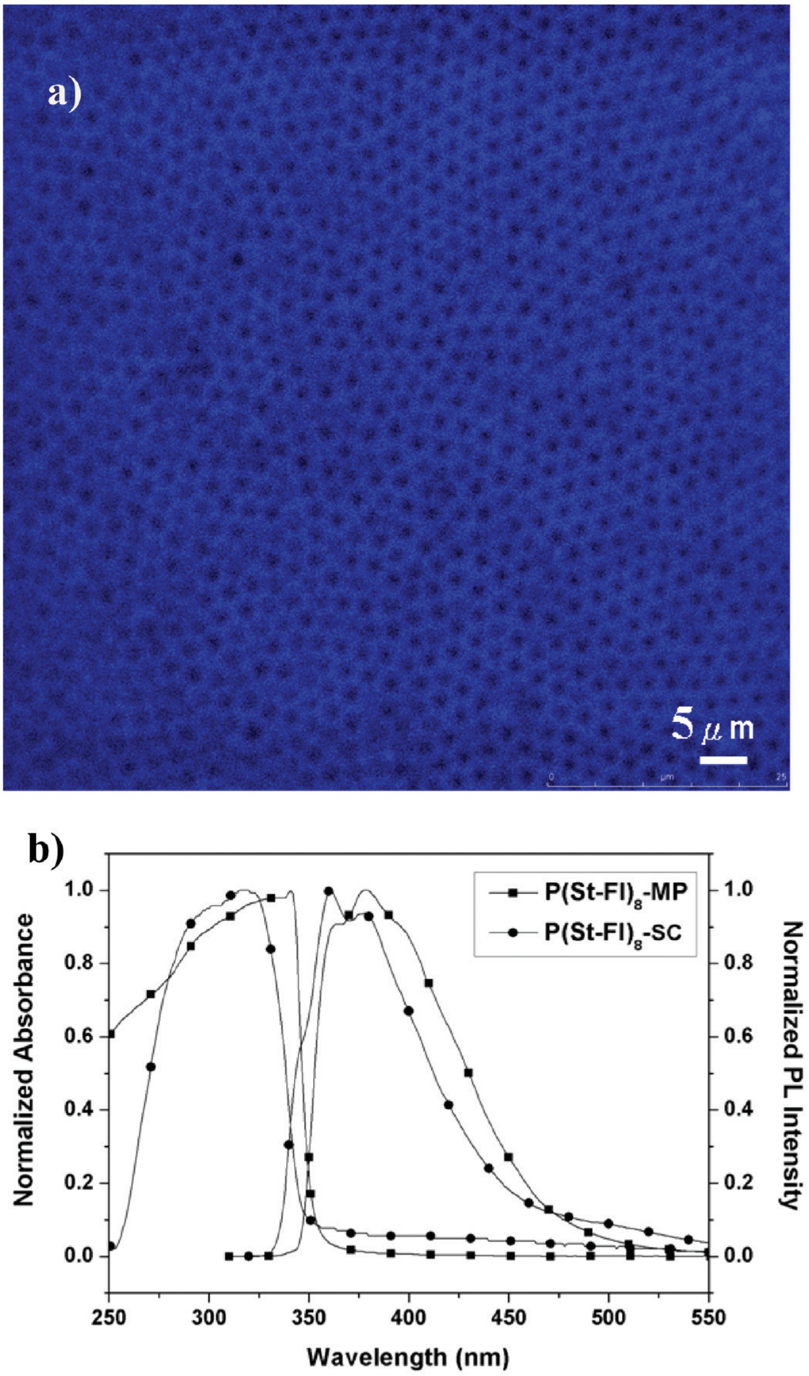

Figure 7. (a) Confocal fluorescence microscopy images of the P(St-Fl)$_8$ microporous film (showing the emission of the fluorescing films between 410 and 500 nm). (b) UV−vis absorption and photoluminescent spectra of the microporous (MP) or spin-casting (SC) P(St-Fl)$_8$ thin films.

envelope to stabilize the water droplet.[32] It thus prevents the coalescence of water droplets and forms the ordered microporous structure when the solvent is completely evaporated. As discussed in the previous paragraph, the polymer architecture and casting condition (such as solvent, concentration, and humidity, etc.) affect the formation of such ordered structure significantly.

Figure 7a shows the confocal microscope images of the P(St-Fl)$_8$, which exhibits the ordered microporous structure with a relatively strong and an uniform blue emission image. Figure 7b shows the absorption and emission thin film spectra of the P(St-Fl)$_8$ films. The photophysical properties of the P(St-Fl)$_8$ microporous (MP) films are different from that of the spin-coated (SC) film. The absorption peak maxima of the studied polymer films are observed at 320 yand 340 nm for the SC and MP films, respectively. The emission maximum (nm) slightly shifts from (361, 378) of the SC film to (365, 379) of the HC film. It indicates that the ordered microporous structure enhances the π-interaction between the polymer chains. In addition, multicolor microporous films were obtained via blending a relatively small amount of conjugated moieties through efficient energy transfer. ADS233YE and Ir(piq)$_2$(acac) were selected as the dopants due to the significant overlapping on their absorption spectrum with the emission spectrum of the P(St-Fl)$_8$. Figure 8 shows the PL spectra of the P(St-Fl)$_8$

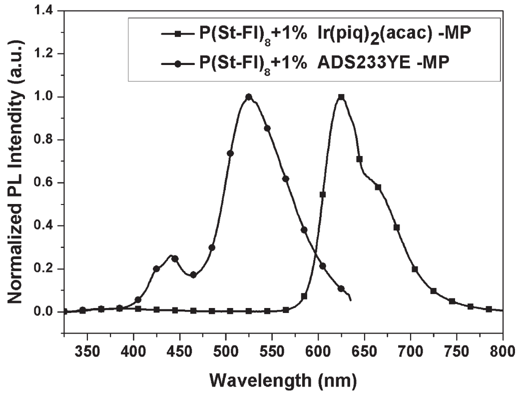

Figure 8. Photoluminescent spectra of P(St-Fl)$_8$ microporous (MP) films blending with 1 wt % ADS233YE or Ir(piq)$_2$(acac).

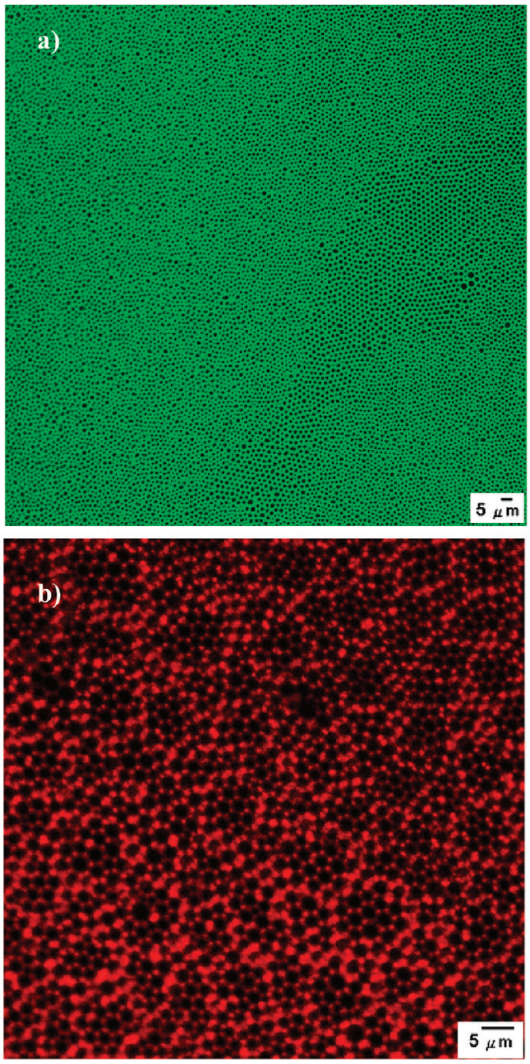

Figure 9. Confocal fluorescence microscopy images of the P(St-Fl)$_8$ microporous thin film blending with 1 wt % (a) ADS233YE (showing the emission of the fluorescing films between 500 and 600 nm) and (b) Ir(piq)$_2$(acac).

HC thin films blended with 1 wt % ADS233YE or 1% Ir(piq)$_2$(acac). The PL peak maxima of P(St-Fl)$_8$ + 1% ADS233YE and P(St-Fl)$_8$ + 1% Ir(piq)$_2$(acac) microporous films are observed at 526 and 624 nm, respectively. The original emission peaks of P(St-Fl)$_8$ at 365 and 379 nm completely disappeared in the blend films despite only 1% of dopant being used, which suggests the significant Foster energy transfer.[33,34] The above result suggests the successful color tuning on the microporous films simply by incorporation of a relatively small different blending materials. Figures 9a and 9b show the confocal microscope images of the P(St-Fl)$_8$ blending with 1 wt % ADS233YE and 1% Ir(piq)$_2$(acac), respectively, which exhibits relatively strong and uniform green and red emission images. The prepared multicolor luminescent microporous films may have the applications in chemical, biological sensor, or molecular electronic devices.

Conclusions

We have successfully synthesized new star-shaped polymers with styrene para-substituted fluorene moieties by living anionic polymerization with multifunctional benzyl bromide core. The experimental results showed that the high molecular weight P(St-Fl)$_8$ could form a highly ordered microporous films via drop-casting, but not for other polymers with lower arm numbers. In addition, the pore diameter was reduced while enhancing solution concentration or decreasing humidity. Relatively uniform blue-emitting characteristic was observed on the P(St-Fl)$_8$ microporous film. Such highly ordered structure led to a red shift in photophysical properties such as absorption and photoluminescence. Furthermore, multicolor microporous films were obtained via blending only 1% of green or red emitter into the P(St-Fl)$_8$ films through efficient energy transfer. The present study suggested novel star-shaped polymer with pendant conjugated moieties could be synthesized by living anionic polymerization and formed the multicolor ordered microporous films.

Acknowledgment. The financial support of this work from National Science Council, The Ministry of Economics Affairs, and the Excellence Research Program of National Taiwan University is highly appreciated. This work was partly supported by a Kakenhi grant (Grant-in-Aid for Scientific Research (B) 21350060) from Japan Society for the Promotion of Science.

Supporting Information Available: GPC trace of P(St-Fl)$_8$ star-shaped polymers; ^{1}H NMR spectra of the P(St-Fl)$_4$ and P(St-Fl)$_8$; TGA and DSC curves of the studied star-shaped polymers under nitrogen atmosphere. SEM image of P(St-Fl) and spin-cast P(St-Fl)$_8$; photographs of P(St-Fl)$_3$, P(St-Fl)$_4$, and P(St-Fl)$_8$ in pure solvents (CS$_2$/water mixed solvent). This material is free of charge via the Internet at http://pubs.acs.org.

References and Notes

(1) Painter, O.; Lee, R. K.; Scherer, A.; Yariv, A.; O'Brien, J. D.; Dapkus, P. D.; Kim, I. *Science* **1999**, *284*, 1819.
(2) Yablonovitch, E. *J. Opt. Soc. Am. B* **1993**, *10*, 283.
(3) Min, E.; Wong, K. H.; Stenzel, M. H. *Adv. Mater.* **2008**, *20*, 3550.
(4) Phillip, W. A.; O'Neill, B.; Rodwogin, M.; Hillmyer, M. A.; Cussler, E. L. *ACS Appl. Interface* **2010**, *2*, 847.
(5) Yabu, H.; Takebayashi, M.; Tanaka, M.; Shimomura, M. *Langmuir* **2005**, *21*, 3235.
(6) Yabu, H.; Hirai, Y.; Kojima, M.; Shimomura, M. *Chem. Mater.* **2009**, *21*, 1787.
(7) Bunz, U. H. F. *Adv. Mater.* **2006**, *18*, 973.
(8) Shrinivasarao, M.; Collings, D.; Philips, A.; Patel, S. *Science* **2001**, *292*, 79.
(9) Widawski, G.; Rawiso, M.; François, B. *Nature* **1994**, *369*, 387.
(10) Stenzel, M. H.; Barner-Kowollik, C.; Davis, T. P. *J. Polym. Sci., Part A: Polym. Chem.* **2006**, *44*, 2363.
(11) Stenzel, M. H. *Aust. J. Chem.* **2002**, *55*, 239.
(12) Heeger, A. J. *Chem. Soc. Rev.* **2010**, DOI: 10.1039/b914956m.
(13) Arias, A. C.; MacKenzie, J. D.; McCulloch, I.; Rivnay, J.; Salleo, A. *Chem. Rev.* **2010**, *110*, 3.
(14) Clarke, T. M.; Durran, J. R. *Chem. Rev.* **2010**, DOI: 10.1021/cr900271s.

(15) Friend, R. H.; Gymer, R. W.; Holmes, A. B.; Burroughes, J. H.; Marks, R. N.; Taliani, C.; Bradley, D. D. C.; Dos Santos, D. A.; Brédas, J. L.; Lögdlund, M.; Salaneck, W. R. *Nature* **1999**, *397*, 121.
(16) Jenekhe, S. A.; Chen, X. L. *Science* **1999**, *283*, 372.
(17) Song, L.; Bly, R. K.; Wilson, J. N.; Bakbak, S.; Park, J. O.; Srinivasarao, M.; Bunz, U. H. F. *Adv. Mater.* **2004**, *16*, 115.
(18) Vamvouis, G.; Nyström, D.; Antoni, P.; Lindgren, M.; Holdcroft, S.; Hult, A. *Langmuir* **2006**, *22*, 3959.
(19) Ejima, H.; Iwata, T.; Yoshie, N. *Macromolecules* **2008**, *41*, 9846.
(20) Govor, L. V.; Bashmakov, A.; Kiebooms, R.; Dyakonov, V.; Parisi, J. *Adv. Mater.* **2001**, *13*, 588.
(21) Barner-Kowollik, C.; Dalton, H.; Davis, T. P.; Stenzel, M. H. *Angew. Chem., Int. Ed.* **2003**, *42*, 3664.
(22) Stenzel-Rosenbaum, M. H.; Davis, T. P.; Fane, A. G.; Chen, V. *Angew. Chem., Int. Ed.* **2001**, *40*, 3428.
(23) Connal, L. A.; Vestberg, R.; Hawker, C. J.; Qiao, G. G. *Adv. Funct. Mater.* **2008**, *18*, 3706.
(24) Wong, K. H.; Hernández-Guerrero, M.; Granville, A. M.; Davis, T. P.; Barner-Kowollik, C.; Stenzel, M. H. *J. Porous Mater.* **2006**, *13*, 213.
(25) Lord, H. T.; Quinn, J. F.; Angus, S. D.; Whittaker, M. R.; Stenzel, M. H.; Davis, T. P. *J. Mater. Chem.* **2003**, *13*, 2819.
(26) François, B.; Pitois, O.; François, J. *Adv. Mater.* **1995**, *7*, 1041.
(27) François, B.; Ederlé, Y.; Mathis, C. *Synth. Met.* **1999**, *103*, 2362.
(28) Hirao, A.; Hayashi, M.; Loykulnant, S.; Sugiyama, K.; Ryu, S. W.; Haraguchi, N.; Matsuo, A.; Higashihara, T. *Prog. Polym. Sci.* **2005**, *30*, 111.
(29) Hirao, A.; Inoue, K.; Higashihara, T.; Hayashi, M. *Polym. J.* **2008**, *40*, 923.
(30) Sugiyama, K.; Hirao, A.; Hsu, J. C.; Tung, Y. C.; Chen, W. C. *Macromolecules* **2009**, *42*, 4053.
(31) Hirao, A.; Matsuo, A.; Watanabe, T. *Macromolecules* **2005**, *38*, 8701.
(32) Kathaus, O.; Maruyama, N.; Cieren, X.; Shimomura, M.; Hasegawa, H.; Hashimoto, T. *Langmuir* **2000**, *16*, 6071.
(33) Fang, Y. K.; Lee, W. Y.; Tuan, C. S.; Teng, W. J.; Chen, W. C. *Polym. J.* **2010**, *42*, 327.
(34) Wu, W. C.; Liu, C. L.; Chen, W. C. *Polymer* **2006**, *47*, 527.